

# Compatibilization of Polyester/Polyamide Blends with a Phosphonated Poly(ethylene terephthalate) Ionomer: Comparison of Monovalent and Divalent Pendant Ions

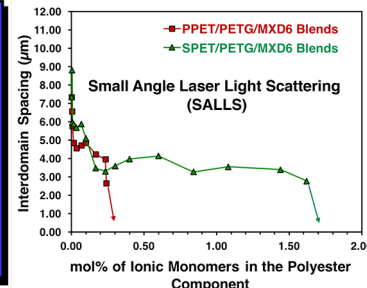
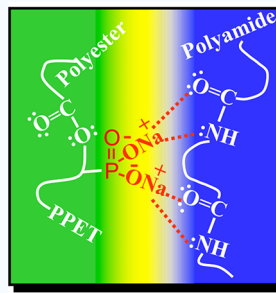
Lin Ju,<sup>id</sup> Joseph M. Dennis, Katherine V. Heifferon, Timothy E. Long,<sup>id</sup> and Robert B. Moore<sup>\*id</sup>

Department of Chemistry, Macromolecules Innovation Institute, Virginia Polytechnic Institute and State University, Blacksburg, Virginia 24061, United States

## Supporting Information

**ABSTRACT:** The successful compatibilization of immiscible amorphous polyester (PETG) and semicrystalline polyamide (poly(*m*-xylylene adipamide) (MXD6)) blends using a phosphonated poly(ethylene terephthalate) ionomer in the  $\text{Na}^+$  form ( $\text{Na}^+$ -PPET) as a minor-component compatibilizer was demonstrated. The  $\text{Na}^+$ -PPET/PETG/MXD6 blends were prepared using a solution mixing method to enable thin film characterization. The phase morphology with respect to various phosphonated monomer concentrations was studied using phase contrast optical microscopy (PC-OM) and small-angle laser light scattering (SALLS). The phase-separated, interdomain spacing decreased with increasing mol % phosphonated monomers and was attributed to the specific interactions between the ionic phosphonate groups on the polyester ionomer and the amide linkages of polyamide. The ability of the divalent phosphonate pendant ions to compatibilize PETG/MXD6 blends was also compared to a conventional sulfonated PET (SPET) compatibilizer. This comparison showed that the  $\text{Na}^+$ -PPET/PETG/MXD6 blends required 6 times fewer ionic monomers to achieve domain dimension  $<1 \mu\text{m}$  as compared to  $\text{Na}^+$ -SPET-containing PETG/MXD6 blends. Moreover, on a mole percent of pendant ions basis, the divalent phosphonate pendant ions in PPET were found to be 3 times more effective at compatibilizing PETG/MXD6 blends compared to the monovalent sulfonate pendant ions in SPET.

**KEYWORDS:** polyester/polyamide blends, compatibilization, phase separation, phosphonated PET ionomer, multivalent ionomer



## INTRODUCTION

Polyester/polyamide blends attract attention in the area of food packaging due to the combination of the low oxygen and carbon dioxide permeability of the polyamide component with good toughness, clarity, and economics of the polyester matrix.<sup>1–6</sup> The broad application of polyester/polyamide blends in gas barrier packaging, however, is often limited by poor optical clarity due to the thermodynamic immiscibility between the two dissimilar polymers.<sup>7,8</sup> Therefore, efforts to enhance the polyester/polyamide compatibility to significantly reduce domain dimensions of the minor polyamide phase within the polyester matrix have remained a priority for many researchers.

Ionomers are charged polymers that contain minor amounts (typically  $<15$  mol %) of covalently attached ionic functionalities incorporated into or pendant to the polymer backbones.<sup>9–11</sup> The functional polymers have proven to be attractive, interfacially active compatibilizers for a number of blend systems because of specific interactions that may develop between the ionic groups and complementary functional groups on other polar polymers within the blend.<sup>12–17</sup> These specific interactions tend to decrease the interfacial tension between the dissimilar polymers, leading to reduced phase

dimensions and enhanced phase stability that inhibits coalescence during melt processing.<sup>18,19</sup> Several ionomers bearing pendant carboxylate or sulfonate ionic groups have been utilized as efficient compatibilizers in immiscible polyester/polyamide blends.<sup>1,3,4,6,12,13,18,20</sup> For example, Kalfolou et al.<sup>20</sup> employed Surlyn, an acrylic-modified polyolefin-type ionomer, to compatibilize a melt-mixed poly(ethylene terephthalate) (PET)/nylon-6 blend. Mechanical tests demonstrated effective compatibilization at ionomer loadings  $>10$  wt % as revealed by increased ductility and enhanced impact strength. Weiss et al.<sup>13</sup> reported the successful compatibilization of liquid crystalline polyester (LCP) with nylon-66 by the incorporation of a zinc-neutralized lightly sulfonated polystyrene ( $\text{Zn}^{2+}$ -SPS) ionomer. The addition of  $\text{Zn}^{2+}$ -SPS to LCP/nylon-66 blend reduced the dispersed-phase size, and the compatibilized blends exhibited significantly enhanced tensile modulus and tensile stress at break compared to the blends without the ionomer. In our earlier work, we proved the enhanced compatibility of an amorphous polyester/polyamide

Received: January 31, 2019

Accepted: April 2, 2019

Published: April 2, 2019

(PETG 6763/Durethan T40) blend with an added amorphous sulfonate polyester ionomer ( $\text{Na}^+$ -SPETG) as a compatibilizer using solution mixing and melt blending methods, as revealed by enhanced dispersion of the minor phase and a significant reduction in the dispersed-phase sizes.<sup>18</sup> Sulfonated poly(ethylene terephthalate) ionomers in  $\text{Na}^+$ -form ( $\text{Na}^+$ -SPET) have also been widely utilized as compatibilizers in melt-mixed polyester/polyamide blends, e.g., poly(ethylene terephthalate) (PET)/poly(*m*-xylylene adipamide) (MXD6) and PET/nylon-6.<sup>1,3,4,6</sup> Both specific interactions and transesterification reactions within SPET-compatibilized polyester/polyamide blends have been demonstrated to play a role in the overall compatibilization process for melt-mixed polyester/polyamide blends.<sup>12</sup>

The ability of an ionomer to effectively compatibilize immiscible polymer blends strongly depends on the counterion type of the ionomer.<sup>12,21–24</sup> Ionomers that are neutralized using divalent counterions can exhibit stronger effects on the compatibility of immiscible polymer blends compared to ionomers with monovalent counterions. For example, MacKnight et al.<sup>21</sup> studied the effect of counterion type on the binary blend system of a metal-neutralized SPET ionomer with poly(ethyl acrylate-*co*-4-vinylpyridine) (EAVP). In contrast to the blends containing monovalent  $\text{Na}^+$  and  $\text{Li}^+$  form SPET ionomers, SPET/EAVP blends containing divalent counterions, such as alkaline earth ( $\text{Ca}^{2+}$ ) and divalent transition metals ( $\text{Co}^{2+}$ ,  $\text{Ni}^{2+}$ ,  $\text{Cu}^{2+}$ , and  $\text{Zn}^{2+}$ ), exhibited enhanced modulus and tensile strength. Similarly, our previous investigation<sup>12</sup> focused on the evaluation of counterion type, e.g.,  $\text{Na}^+$ ,  $\text{Mn}^{2+}$ , and  $\text{Zn}^{2+}$ , of an amorphous polyester ionomer (AQ 55) on the degree of compatibility for AQ 55/nylon-66 blends. The blends with AQ ionomer in the divalent form showed superior compatibility (i.e., larger  $T_m$  depression and enhanced dispersion of the minor phase), in contrast to the monovalent analogues.

As alternative pendant groups, phosphonated monomer units have been relatively under represented in the ionomer literature. Weiss et al.<sup>25</sup> reported the viscoelastic properties of poly(styrene-*co*-vinylphosphonate) ionomers in a variety of counterion forms. In the field of polymer blends, Pearce and co-workers<sup>26</sup> found that polystyrene containing pendant phosphonic acid groups were immiscible with poly(*n*-butyl methacrylate). Despite the well-studied effect of polyester ionomer counterion type on the compatibility of immiscible polymer blends, no systematic studies have been focused on an investigation of multivalent pendant ions in polyesters, such as the divalent phosphonate pendant ion. Recently, we synthesized phosphonated PET ionomers in the  $\text{Na}^+$ -form ( $\text{Na}^+$ -PPET) by melt polycondensation reaction and reported their thermal, rheological, and mechanical properties.<sup>27</sup> As an alternative compatibilizer to the widely used  $\text{Na}^+$ -SPET ionomer, the  $\text{Na}^+$ -PPET ionomer bearing divalent pendant ions is potentially an attractive candidate for polyester/polyamide blends. Monovalent sulfonate ion pairs are known to interact strongly with the amide linkages,<sup>22</sup> thus establishing an interphase of specific interactions (Figure 1A).<sup>15</sup> It is postulated that the divalent phosphonate pendant ions are capable of generating stronger specific interactions per functional monomer unit (Figure 1B) that could provide a more effective mode of compatibilization in polyester/polyamide blends as compared to a polyester ionomer bearing monovalent sulfonate pendant ions. In this work, we report the first investigation of the compatibilization of polyester/

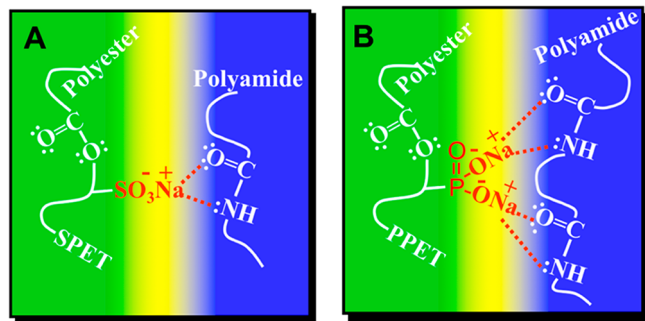


**Figure 1.** Schematic representations for the specific interactions between the pendant ions and amide linkages of the polyamide in polyester/polyamide blends. (A) Monovalent sulfonate pendant ion. (B) Postulated interactions with the divalent phosphonate pendant ion.

polyamide blends with a  $\text{Na}^+$ -PPET ionomer along with a direct comparison of monovalent sulfonate and divalent phosphonate pendant ions on the compatibilization of polyester/polyamide blends.

## EXPERIMENTAL SECTION

**Materials.** 1,1,1,3,3-Hexafluoro-2-propanol (HFIP,  $\geq 99.5\%$ ) was purchased from Acros Organics and used as received. The amorphous polyester (PETG 6763) composed of terephthalic acid and ethylene glycol with a portion of the glycol units substituted with cyclohexane-dimethanol was supplied by Eastman Chemical Company. Poly(*m*-xylylene adipamide) (MXD6) was supplied by Mitsubishi Gas Chemical Co., and sulfonated poly(ethylene terephthalate) ionomers in  $\text{Na}^+$ -form ( $\text{Na}^+$ -SPET) with 1.80 mol % terephthalate replaced with sodium 5-sulfoisophthalate was obtained from Eastman Chemical Co. Phosphonated poly(ethylene terephthalate) ionomer in  $\text{Na}^+$ -form ( $\text{Na}^+$ -PPET) with 0.5 mol % 5-phosphoisophthalate units randomly distributed along the polymer chain was synthesized by melt polycondensation reaction as described in our recent publication.<sup>27</sup>

**Preparation of Solution Blends.** All blends were prepared as 1.5% (w/v) solutions in HFIP. To prepare the blends,  $\text{Na}^+$ -PPET ionomer was first dissolved in HFIP, and the solution was allowed to stir for 48 h at 60 °C to ensure complete dissolution and mixing. PETG/MXD6 solutions were obtained by dissolving various ratios of PETG and MXD6 in 2 mL of HFIP at 60 °C after stirring for about 3 h. The  $\text{Na}^+$ -PPET/PETG/MXD6 solution blends were prepared by combining the appropriate  $\text{Na}^+$ -PPET and PETG/MXD6 solutions to achieve the desired blend compositions (specifically focusing on the mol % of ionic monomers), as listed in Table 1. The generated solution blends were allowed to stir at 60 °C for 24 h to ensure complete dissolution and mixing. The blend compositions were designated as wt % polyester matrix (mol % of phosphonated monomers in the polyester component)/wt % MXD6.  $\text{Na}^+$ -SPET/PETG/MXD6 blends with the same mol % of ionic monomers as in the  $\text{Na}^+$ -PPET/PETG/MXD6 blends were also prepared by the same procedure.

**Solution Casting Method.** To prepare thin film blend specimens,  $<10\ \mu\text{m}$  thick, suitable for characterization by phase contrast optical microscopy (PC-OM) and small-angle laser light scattering (SALLS), 0.05 mL of the solution blends was cast onto microscope slides at room temperature. Then, the wet film was covered using an inverted 20 mL glass vial and allowed to dry for  $\sim 15$  min at room temperature to generate a uniform film (i.e., without observed defects or air bubbles). The same film casting process was utilized to prepare the  $\text{Na}^+$ -SPET/PETG/MXD6 solution blends.

**Phase Contrast Optical Microscopy (PC-OM).** The phase morphology of the solution-cast films was characterized using a Nikon Eclipse LV100 microscope equipped with a Linkam TMS 94 hot stage and a Linkam LNP temperature controller. A Nikon digital camera (DXM1200) was utilized for image acquisition. The optical

Table 1. PETG/Na<sup>+</sup>-PPET/MXD6 Blend Compositions

	composition <sup>a</sup>	wt % PETG	wt % 0.5Na <sup>+</sup> -PPET	wt % MXD6	mol % of ionic monomer <sup>b</sup>	stoichiometry <sup>c</sup>
A	75 (0.000)/25	75	0	25	0	0
B	75 (0.0033)/25	74.5	0.5	25	0.00333	0.000064
C	75 (0.0067)/25	74	1	25	0.00667	0.00013
D	75 (0.0133)/25	73	2	25	0.0133	0.00026
E	75 (0.0333)/25	70	5	25	0.0333	0.00064
F	75 (0.0667)/25	65	10	25	0.0667	0.0013
G	75 (0.100)/25	60	15	25	0.100	0.0019
H	75 (0.167)/25	50	25	25	0.167	0.0032
I	75 (0.233)/25	40	35	25	0.233	0.0045
J	75 (0.240)/25	39	36	25	0.240	0.0046
K	75 (0.247)/25	38	37	25	0.247	0.0058
L	75 (0.300)/25	30	45	25	0.300	0.0077

<sup>a</sup>Blend compositions are designated as wt % polyester matrix (mol % of phosphonated monomers in the polyester component)/wt % MXD6. <sup>b</sup> mol % of phosphonated monomers in the polyester component. <sup>c</sup>Molar ratio of phosphonated monomers to amide units in the MXD6 component.

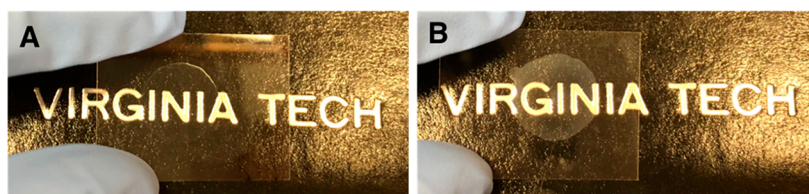


Figure 2. PETG/MXD6 base blend film on a microscope slide. (A) Transparent as-cast film at room temperature and (B) translucent film after rapid cooling from the melt (240 °C held for 10 s) to room temperature.

microscope was used in phase contrast mode with a 10× Ph1 objective, and the polarizer was removed. The as-cast film was heated to 240 °C (50 °C/min) and held at this temperature for 10 s to allow for complete melting of the Na<sup>+</sup>-PPET and MXD6 crystallites and possible liquid–liquid phase separation. The phase-separated morphology was observed after the film was rapidly cooled to room temperature. The interdomain spacing was measured using ImageJ. For each blend composition, the mean  $\pm \sigma$  value was calculated from 200 measurements by fitting a histogram of the measurements to a Gaussian distribution.

**Small-Angle Laser Light Scattering (SALLS).** The same heat-treated films analyzed by PC-OM were utilized in the small-angle laser light scattering (SALLS) experiment. The incident light was obtained from a 3 mW He–Ne laser ( $\lambda = 632.8$  nm, Oriel Corp., model 6697). The scattered  $V_v$  (i.e., the polarizer in the incident beam and the analyzer in the scattered beam are in parallel orientations) pattern was projected onto a detector plane (i.e., a sheet of white paper) that was positioned at a set distance from the sample stage. The digital image on the detector plane was captured using a Photometrics SenSys 1401E CCD camera interfaced with a computer. The sample-to-detector distance (SDD) was 30 cm, and the  $q$ -range, where  $q$  is the scattering vector, was calibrated using a 300 lines/mm diffraction grating. All SALLS data were analyzed using the Rigaku SAXSGUI software package to obtain radially integrated SALLS intensity versus scattering vector  $q$  profiles. The experimental interdomain spacing,  $d$ , was obtained at the maximum intensity, and the corrected interdomain spacing,  $d'$ , was calculated by compensating for the refractive indices of PETG and MXD6 according to eqs 1 and 2:<sup>18,28,29</sup>

$$d = \frac{n_1 \lambda}{2 \sin(\theta/2)} \quad (1)$$

$$d' = \frac{1.025 \lambda / n_2}{\pi \sin(\theta'/2)} \quad (2)$$

where  $n_1$  is the order of reflection ( $n_1 = 1$ ),  $\lambda$  is the wavelength of incident light ( $\lambda = 632.8$  nm),  $\theta$  and  $\theta'$  are the experimentally observed and the corrected scattering angles at maximum intensity,

respectively, and  $n_2$  is the blend sample refractive index. The scattering angle was corrected for refraction at the sample surface by the formula  $n_2 = \sin \theta / \sin \theta'$ . The value of  $n_2$  was calculated according to the relationship  $n_2 = n_{\text{PETG}} \times \text{wt \% of polyester} + n_{\text{MXD6}} \times \text{wt \% of polyamide}$ , where  $n_{\text{PETG}} = 1.567$  and  $n_{\text{MXD6}} = 1.577$ .<sup>8,30</sup>

**Fourier Transform Infrared Spectroscopy (FTIR).** As a model study, four MXD6/ionic monomer blends with 40 and 60 mol % sulfonated (i.e., sodium 5-sulfoisophthalate) and phosphonated ionic monomers (i.e., sodium 5-phosphoisophthalate) to amide monomer units of MXD6 were prepared as 1.2% (w/v) solutions in HFIP. To prepare the mixtures, MXD6 and ionic monomers were dissolved in HFIP and allowed to stir for 12 h at 60 °C to ensure complete dissolution and mixing. The MXD6/ionic monomer mixtures were obtained by removal of HFIP under ambient pressure (1 atm) at 50 °C and further vacuum drying for 12 h at 50 °C. FTIR was performed on the resulting solids using a Varian 670-IR spectrometer with a DTGS detector using the Pike Technologies GladiATR attachment (diamond crystal). Spectra were collected as the average of 32 scans at 4  $\text{cm}^{-1}$  resolution.

**Differential Scanning Calorimetry (DSC).** A TA Instruments Q2000 DSC was used to determine the thermal transitions and crystallization behavior of the Na<sup>+</sup>-PPET/PETG/MXD6 blends, tabulated in Table S1. Samples were predried at 50 °C for 12 h before DSC tests. Under a nitrogen atmosphere, the samples (~5–8 mg) were heated from 0 to 270 °C at 10 °C/min, quenched to 0 °C at –60 °C/min, reheated from 0 to 270 °C at 10 °C/min, and then cooled to 0 °C at –10 °C/min. The glass transition temperature ( $T_g$ ), melting temperature ( $T_m$ ), and enthalpy of melting ( $\Delta H_m$ ) were determined from the second heating scan after erasing the thermal history; the crystallization temperature ( $T_c$ ) and enthalpy of crystallization ( $\Delta H_c$ ) were investigated from the subsequent cooling scan by using the TA Instruments Universal Analysis software.

## RESULTS AND DISCUSSION

**Phase Morphology of the PETG/MXD6 Blend.** Blends of PETG and MXD6 (composition A, without compatibilizer) are termed the base blend in this study. Figure 2 shows images of the as-cast PETG/MXD6 blend film and the film after rapid

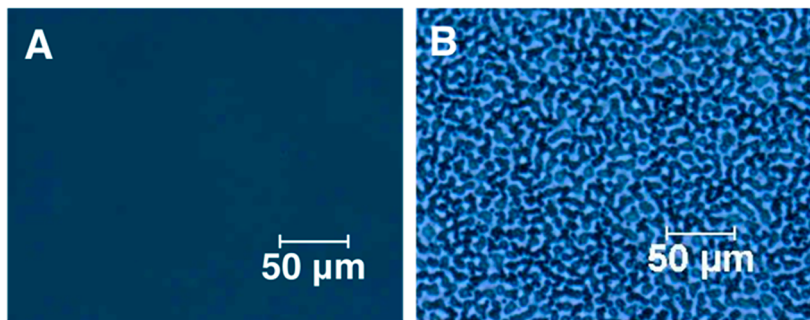


**Figure 3.** Phase contrast optical microscopy (PC-OM) images of the PETG/MXD6 (75/25) base blend. (A) As-cast film at room temperature and (B) after rapid cooling from the melt (240 °C held for 10 s) to room temperature.

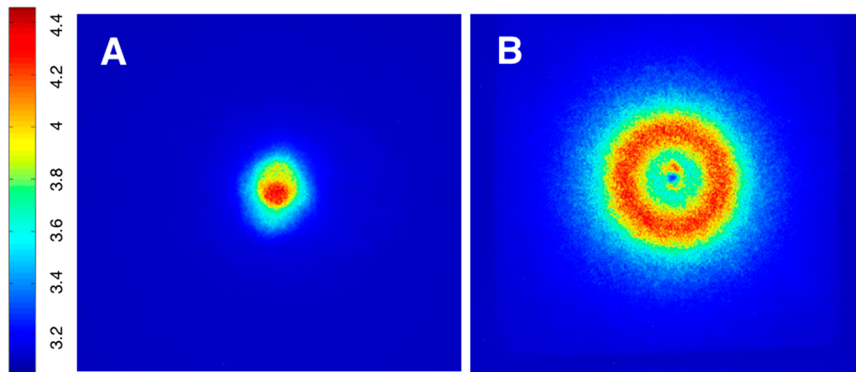


**Figure 4.**  $V_v$  small-angle laser light scattering patterns of the PETG/MXD6 (75/25) base blend. (A) As-cast film at room temperature and (B) after rapid cooling from the melt (240 °C held for 10 s) to room temperature. The sample-to-detector distance (SDD) is 30 cm.

cooling from the melt (240 °C held for 10 s) to room temperature. When the blend of PETG and MXD6 was cast from solution, the resulting thin film was optically transparent (Figure 2A). Upon heating the blend film to 240 °C (i.e., above the melting temperature ( $T_m$ ) of the MXD6 component of 236 °C), the film became visibly translucent, and this translucence remained after rapid cooling to room temperature (Figure 2B). As with most amorphous polymer blends, opacity is generally considered to be indicative of a phase-separated morphology and is attributed to light scattering from the blend domains of dimensions comparable to or greater than the wavelength of visible light having distinctly different refractive indices.<sup>31</sup> While MXD6 is crystallizable, and spherulitic development in a semicrystalline polymer can also produce opacity, it is important to note that the opacity noted here was observed above the  $T_m$  of MXD6, and no spherulites were observed in the cooled samples. Therefore, this translucence is consistent with the expected immiscibility of the PETG/MXD6 blends.

The phase morphology of the solution-cast PETG/MXD6 (75/25) base blend was initially investigated by phase contrast optical microscopy (PC-OM). The optical micrographs of the as-cast PETG/MXD6 base blend film at room temperature and after rapid cooling from 240 °C to room temperature are displayed in Figure 3. The featureless optical micrograph of the as-cast film (Figure 3A) is attributed to a kinetically trapped, homogeneous state of excessive molecular mixing resulting from the relatively rapid solvent evaporation of the blend solution at a temperature well below the glass transition temperatures of the blend components.<sup>32</sup> As opposed to the featureless optical micrograph for the as-cast PETG/MXD6 blend, the film heated to 240 °C exhibits a well-developed

domain morphology (Figure 3B) that is characteristic of thermally induced phase separation by spinodal decomposition.<sup>33</sup> This behavior strongly suggests that liquid–liquid phase separation has taken place above the  $T_m$  of MXD6. Moreover, the phase-separated structure persists upon rapidly cooling the film to room temperature (Figure 3B). Consistent with the translucence observed from the image of melt-treated film (Figure 2B), these data confirm that PETG is immiscible with MXD6, which yields phase-separated domains with dimensions on the order of micrometers.

While PC-OM provides a means for real space analysis of specific domain dimensions in a phase-separated blend (see below), small-angle laser light scattering (SALLS) is a complementary technique to analyze the global dimensions of structural features in reciprocal space.<sup>18,33–35</sup> The formation of phase-separated structures in a polymer blend is revealed as a scattering halo in the SALLS experiment. The size of the halo is inversely proportional to the global average center-to-center interdomain spacing of the phase-separated blend at a constant sample-to-detector distance (SDD). Thus, SALLS is often utilized together with PC-OM to fully characterize the morphology and phase separation behavior of various blend systems.

Figure 4 shows the  $V_v$  scattering patterns for the as-cast and melt-treated PETG/MXD6 (75/25) blend film. In agreement with the PC-OM results (above), no scattering halo is observed in the SALLS patterns of the as-cast PETG/MXD6 blend film at room temperature, again attributed to the excessive mixing of the blend components during solvent casting (Figure 4A). In contrast, the melt-treated blend film shows a distinct scattering halo, which is attributed to the phase-separated morphology of the immiscible blend (Figure

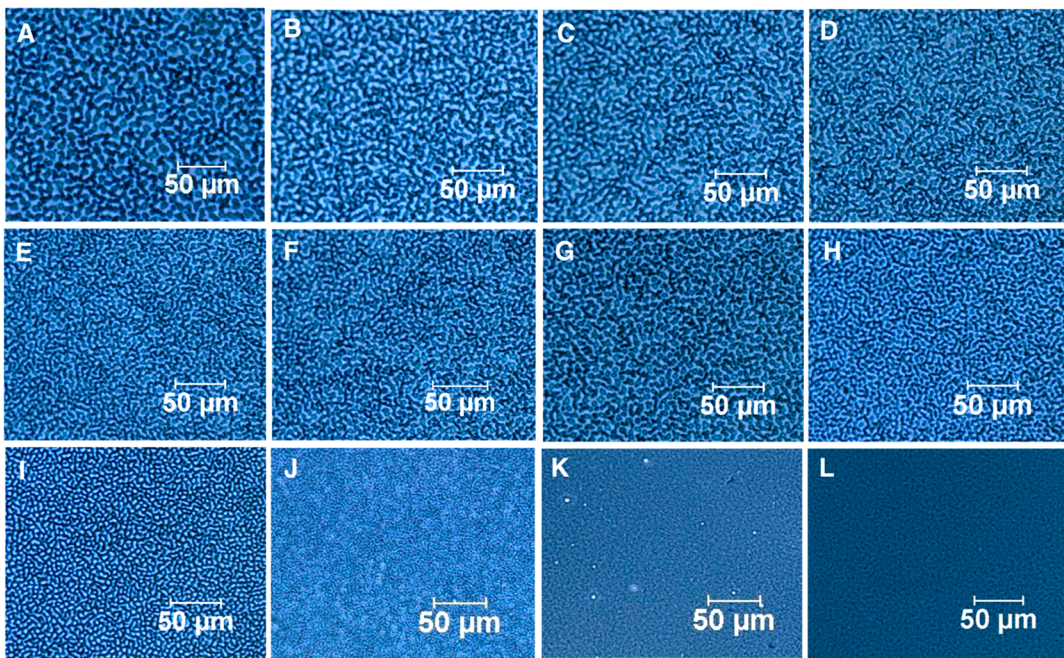


**Figure 5.** Phase contrast optical microscopy (PC-OM) images of the  $\text{Na}^+$ -PPET/PETG/MXD6 blends: (A) 75 (0.000)/25; (B) 75 (0.00333)/25; (C) 75 (0.00667)/25; (D) 75 (0.0133)/25; (E) 75 (0.0333)/25; (F) 75 (0.0667)/25; (G) 75 (0.100)/25; (H) 75 (0.167)/25; (I) 75 (0.233)/25; (J) 75 (0.240)/25; (K) 75 (0.247)/25; (L) 75 (0.300)/25. Scale bar = 50  $\mu\text{m}$ .

4B). This behavior is consistent with the spinodal structure induced by the phase separation process.

**Investigation of  $\text{Na}^+$ -PPET Ionomer-Compatibilized PETG/MXD6 Blends by Phase Contrast Optical Microscopy (PC-OM).** The compatibilization effect of the phosphonate pendant ions in  $\text{Na}^+$ -PPET on the phase behavior of PETG/MXD6 blends was investigated using PC-OM. The optical micrographs for  $\text{Na}^+$ -PPET/PETG/MXD6 blends after rapid cooling from the melt (240 °C held for 10 s) with various amounts of phosphonate groups are shown in Figure 5. The ternary  $\text{Na}^+$ -PPET/PETG/MXD6 blends (Figure 5B–J) exhibit the same spinodal structure as the binary PETG/MXD6 control (base blend, Figure 5A). As the mol % of ionic phosphonated monomers increases, the dispersed-phase dimensions are reduced (see Figures S1 and S2). For the blends with 0.247 mol % ionic phosphonated monomers and higher, phase-separated domains are not clearly observed within the contrast and resolution limits of this optical microscopy technique. The significant loss of contrast for the blends containing 0.247 mol % ionic phosphonated monomers and higher is indicative of nearly identical refractive indices of the small phases (if present) and is attributed to significant phase mixing between the polyester and polyamide components (Figure 5K,L).

As highlighted in Figure 1B, the phosphonate pendant ions are postulated to serve as sites of specific interactions with the polyamide component that decrease the interfacial tension between the PETG and MXD6 blend components and increase interfacial adhesion,<sup>18,19,36</sup> thus leading to a reduction in the phase-separated domain sizes and an improved interphase mixing. To gain molecular-level insight into the nature of the compatibilization phenomenon, FTIR was used to spectroscopically probe the specific interactions between the pendant ions and amide groups. Because the ionic group content in these blends was extremely low (Table 1), a model study involving a mixture of MXD6 with the functional

monomers at relatively high concentrations was conducted (Figures S3–S5). Consistent with previous studies of ionomer interactions with polyamides,<sup>15</sup> the phosphonate groups of PPET appear to interact with the amide functionalities of MXD6, causing a shift of the amide II band to higher frequencies (Figure S3). In addition, consistent with the work of Lu and Weiss<sup>37</sup> as well as Gemeinhardt et al.,<sup>18</sup> the phosphonate/amide interactions are observed to disrupt the H-bonding of the amide groups, causing an appearance of a band attributed to free N–H units at 3550  $\text{cm}^{-1}$  (Figures S4 and S5). Interestingly, this band at 3550  $\text{cm}^{-1}$  is pronounced for the phosphonate system, while virtually absent for the sulfonate analogue. This observation agrees with the recent findings of Pike et al.,<sup>38</sup> which showed that phosphonate anions are stronger hydrogen-bond acceptors than sulfonate anions. Thus, these results suggest that the phosphonate groups on the  $\text{Na}^+$ -PPET ionomer interact with the amide groups of MXD6 to yield an effective compatibilization of the PETG/MXD6 blend.

While the decrease in phase dimensions with increasing phosphonate content and apparent phase mixing at relatively high  $\text{Na}^+$ -PPET contents is consistent with the concept of ionomer compatibilization in these blends, it should be noted that the phase dimensions observed in Figure 5 are not necessarily equilibrium morphologies. As shown in Figure S6, the phase dimensions of the base blends (without compatibilizer) and the  $\text{Na}^+$ -PPET (0.0667 mol %)-compatibilized blends remain constant over a period of 5 s–4 min (i.e., a time frame consistent with conventional melt-processing). Even at higher temperatures (e.g., up to 280 °C, Figure S7), only a minimal increase in phase dimensions of the base blend is observed. However, at longer times up to 5 h, the dimensions of both systems tend to increase slightly with continued annealing (Figures S8 and S9, respectively), although significantly diminished for the  $\text{Na}^+$ -PPET-compatibilized blend. At relatively high  $\text{Na}^+$ -PPET contents (e.g.,

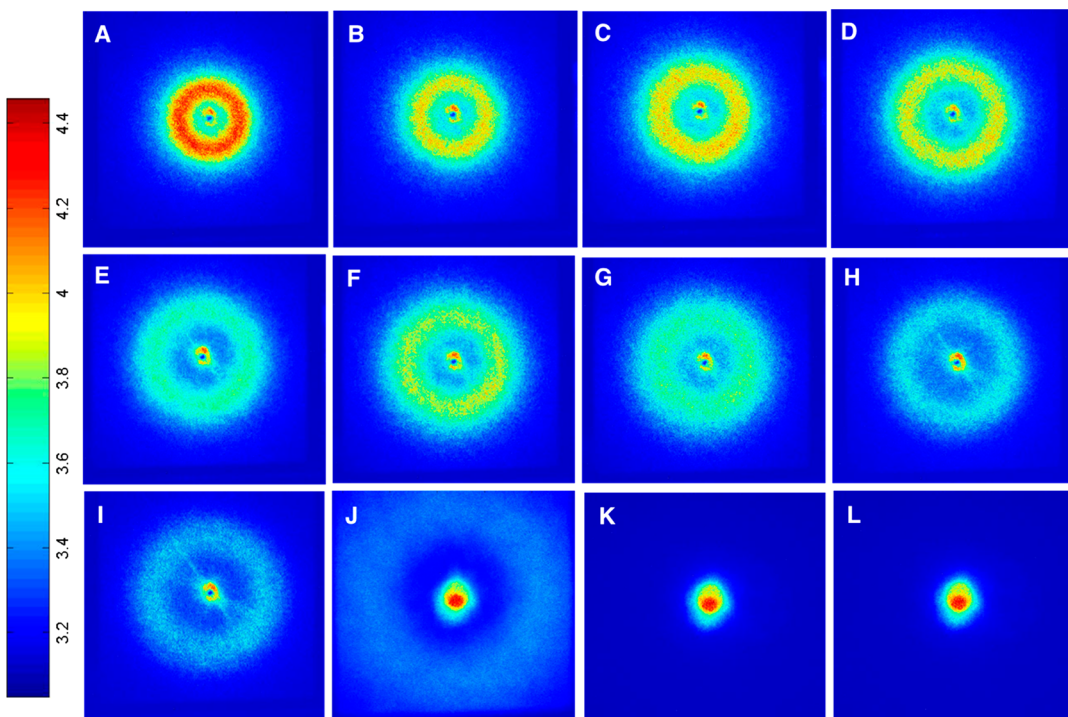


**Figure 6.**  $V_v$  small-angle laser light scattering (SALLS) patterns of the  $\text{Na}^+$ -PPET/PETG/MXD6 blends: (A) 75 (0.000)/25; (B) 75 (0.00333)/25; (C) 75 (0.00667)/25; (D) 75 (0.0133)/25; (E) 75 (0.0333)/25; (F) 75 (0.0667)/25; (G) 75 (0.100)/25; (H) 75 (0.167)/25; (I) 75 (0.233)/25; (J) 75 (0.240)/25; (K) 75 (0.247)/25; (L) 75 (0.300)/25. The sample-to-detector distance (SDD) is 30 cm.

0.233 mol %, Figure S10), the phase dimensions remain constant out to 5 h, consistent with pinned morphologies<sup>16,39,40</sup> attributed to ion-pair associations in the melt. Nevertheless, given the tendency for the easily oxidizable MXD6 to degrade at high temperatures (e.g., discoloration was observed at long annealing times), we have chosen in this study to compare phase dimensions at relatively short annealing times.

**Investigation of  $\text{Na}^+$ -PPET Ionomer-Compatibilized PETG/MXD6 Blends by Small-Angle Laser Light Scattering (SALLS).** SALLS was utilized to provide further insight into the effect of  $\text{Na}^+$ -PPET ionomer on the phase behavior of PETG/MXD6 blends. Figure 6 displays the  $V_v$  SALLS patterns for the set of  $\text{Na}^+$ -PPET/PETG/MXD6 blends. Note that these scattering patterns were acquired based on a constant SDD of 30 cm. At a phosphonated monomer concentration lower than 0.247 mol %, each blend film shows a halo scattering pattern, typical of phase separation in polymer blends. As the mol % of phosphonated monomers increases, the size of the scattering halo increases (i.e., the scattering halo shifts to larger scattering angles). As the size of the halo is inversely proportional to the interdomain spacing of the phase-separated blend at a constant SDD,<sup>18</sup> the larger halo size is evident of a shorter interdomain spacing. For the compositions with 0.247 and 0.300 mol % of ionic monomers, no detectable scattering halo is observed, even at lower SDDs. This undetectable scattering halo further confirms a profound interphase mixing (Figure 6K,L). Moreover, for Figure 6A–J, the scattered intensity diminishes with increased ionic monomer concentration, suggesting a diminishing contrast with increased phase mixing. As a complement to the PC-OM results, these SALLS data reveal significant phase mixing with added sodium phosphonate content and further confirm the

enhanced compatibility of PETG/MXD6 blends with the incorporation of the  $\text{Na}^+$ -PPET ionomer.

To quantify the phase-separated domain dimensions using SALLS, the experimental interdomain spacing for each  $\text{Na}^+$ -PPET/PETG/MXD6 blend was obtained by the procedure described in the [Experimental Section](#) and found to be in excellent agreement with the measured results from PC-OM (Figure S2). Figure 7 shows the dependence of the average

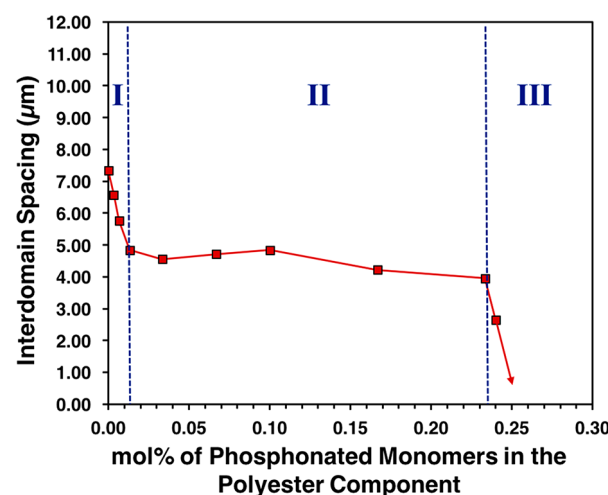


**Figure 7.** Average interdomain spacing of the  $\text{Na}^+$ -PPET/PETG/MXD6 blends calculated from small-angle laser light scattering (SALLS) experiments as a function of phosphonated monomer concentration in the polyester component. Region I: below 0.0133 mol %, where domain size rapidly decreases. Region II: 0.0133–0.233 mol %, where domain size remains relatively constant. Region III: above 0.233 mol %, where rapid loss of scattering is observed.

interdomain spacing on the phosphonated monomer concentration in the polyester component. The interdomain spacings may be divided into three distinct regions: an initial region at low phosphonated monomer concentration, where interdomain spacing decreases greatly with increasing phosphonated monomer concentration (region I), followed by a broad range of phosphonated monomer concentrations between 0.0133 and 0.233 mol % (region II), where interdomain spacing values remain relatively constant. Finally, at phosphonated monomer concentration above 0.233 mol % (region III), a rapid decline in domain dimensions is observed, followed by the loss of a detectable phase morphology.

During the initial stage of increasing phosphonated monomer concentration, corresponding to region I (i.e., below 0.0133 mol %), it is clear that very small amounts of ionic phosphonate groups incorporated to the polyester/polyamide blend system can significantly decrease the phase-separated domain dimensions. For example, with only 0.0133 mol % phosphonated monomers, the interdomain spacing has been reduced by 39% (i.e., from 9.26 to 5.66  $\mu\text{m}$ ). The plateau of relatively constant phase dimensions observed in region II demonstrates that further increasing the mol % of phosphonated monomers has little effect on the interdomain spacing. In region III, the plot begins a steep decline from 5.26 to 2.80  $\mu\text{m}$  as the amount of phosphonated monomers increases from 0.233 to 0.240 mol %. Above 0.240 mol % phosphonated monomer concentration, the domain dimensions suddenly drop below a 1  $\mu\text{m}$  resolution limit such that the distinct domain structure is no longer observed by optical microscopy (Figure 5K,L). From an applied perspective, this “cliff” in composition signifies a transition to a highly compatibilized blend capable of forming domains on a size scale comparable to the wavelength of visible light (e.g., dimensions needed to minimize haze from scattered light in packaging applications.) From a more fundamental perspective, the transitions between the three regions of composition may involve a complex interplay between ionic aggregation (i.e., strong associations between ion pairs, characteristic of ionomers<sup>41</sup>) and the ion–amide associations responsible for compatibilization. Clearly, further investigations will be required to confirm and discriminate the relative contributions of these competing interactions.

**Comparison of the Monovalent Sulfonate and Divalent Phosphonate Pendant Ions.** Given the widespread application of sulfonated PET (SPET) in polymer blend compatibilization,<sup>1,4,12,18</sup> it is of interest here to systematically compare the relative effectiveness of the monovalent sulfonate and divalent phosphonate pendant ions on the phase morphology of PETG/MXD6 blends. In this comparison,  $\text{Na}^+$ -SPET/PETG/MXD6 blends were prepared to contain the same mol % of ionic monomers in the polyester component as that of the  $\text{Na}^+$ -PPET/PETG/MXD6 blends. Given that the functionalized monomer in the PPET copolymer contains twice the number of pendant ions as that of the SPET comonomer, this analysis will show a comparison based on (1) the mol % of ionic monomers in the polyester component as well as (2) a comparison based on the mol % of pendant ions in the blend.

The interdomain spacings obtained from PC-OM (Figure 8A) and SALLS (Figure 8B) for  $\text{Na}^+$ -SPET/PETG/MXD6 and  $\text{Na}^+$ -PPET/PETG/MXD6 blends are compared with respect to the mol % of ionic monomers. The PC-OM images, histograms with Gaussian distribution fits, and the SALLS

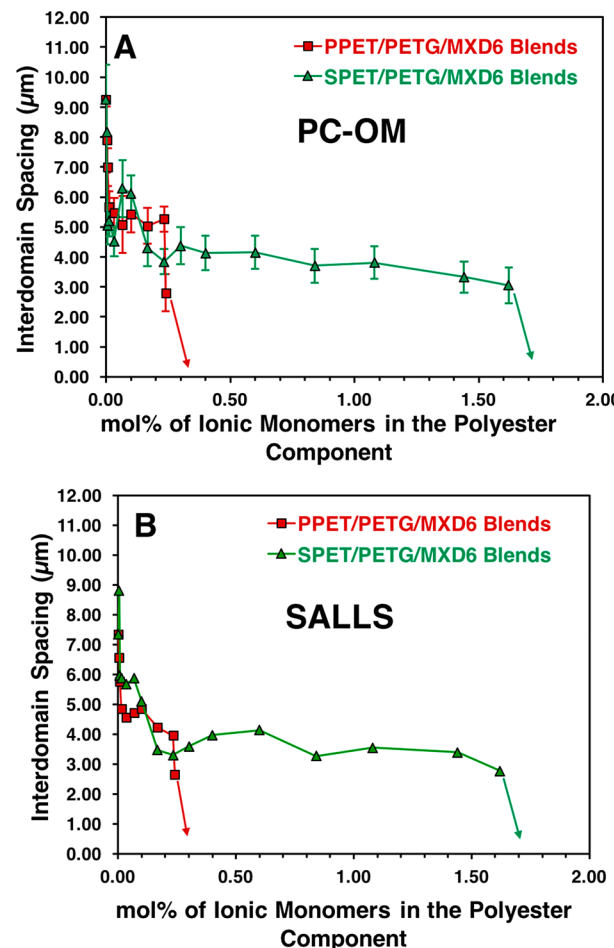


**Figure 8.** Interdomain spacing with respect to mol % of ionic monomers in the polyester component for the  $\text{Na}^+$ -SPET/PETG/MXD6 and  $\text{Na}^+$ -PPET/PETG/MXD6 blends based on (A) measured values from the phase contrast optical microscopy (PC-OM) images and (B) calculated values from small-angle laser light scattering (SALLS).

patterns for  $\text{Na}^+$ -SPET/PETG/MXD6 blends are provided in the Figures S11, S12, and S13, respectively. Interestingly, the general interdomain spacing versus mol % ionic monomer plots of the  $\text{Na}^+$ -SPET/PETG/MXD6 blends follows a similar profile to that of the  $\text{Na}^+$ -PPET ionomer-compatibilized PETG/MXD6 blends, where three distinct regions of phase behavior are evident. This similar observation of the three-region behavior (described above) suggests that the ionic associations responsible for ionomer compatibilization is rather general and not unique to PPET.

At low ionic monomer concentration, i.e., below 0.240 mol %,  $\text{Na}^+$ -PPET ionomer-compatibilized PETG/MXD6 blends exhibit comparable interdomain spacing to that of  $\text{Na}^+$ -SPET/PETG/MXD6 blends, indicating similar compatibilization effect on PETG/MXD6 blends. In distinct contrast, however, the plateau region for  $\text{Na}^+$ -PPET/PETG/MXD6 blends, i.e., 0.0133–0.233 mol %, is 85% shorter than the very broad range of 0.167–1.62 mol % observed for  $\text{Na}^+$ -SPET/PETG/MXD6 blends. In the range of ionic monomer concentration higher than 0.240 mol %, no detectable spinodal structure is observed for  $\text{Na}^+$ -PPET/PETG/MXD6 blends; meanwhile,  $\text{Na}^+$ -SPET ionomer-compatibilized blends still show phase-separated domains with interdomain spacing approximately ranging

from 3.2 to 4.2  $\mu\text{m}$ . The ionic monomer concentration where the steep decline occurs for  $\text{Na}^+$ -PPET ionomer-containing blends is 0.233 mol %, which is 86% lower than the 1.62 mol % for  $\text{Na}^+$ -SPET/PETG/MXD6 blends. This comparison reveals that the  $\text{Na}^+$ -PPET/PETG/MXD6 blends require 6 times fewer ionic monomers to achieve domain dimension  $<1\ \mu\text{m}$  as compared to  $\text{Na}^+$ -SPET-containing PETG/MXD6 blends. Thus, it appears that the divalent phosphonate groups generate stronger specific interactions per functional monomer unit as compared to the monovalent sulfonate pendant ions and consequently a more effective compatibilization in polyester/polyamide blends. From a practical perspective, the superior compatibilization with PPET requires less ionic monomers to achieve the same compatibility of polyester/polyamide blends than that of the conventional SPET-compatibilized blends.

The comparison of interdomain spacings for the  $\text{Na}^+$ -SPET/PETG/MXD6 blends and  $\text{Na}^+$ -PPET/PETG/MXD6 blends on mol % of pendant ions basis is shown in Figure 9. This comparison, while of course involving the same set of data as for Figure 8, highlights the fundamental difference between phosphonate and sulfonate ions, on a per ion basis. At low ion concentrations ( $<0.5\ \text{mol}\%$ ), it appears that the sulfonate ions are slightly more effective at reducing phase dimensions compared to the phosphonate ions. Our recent viscoelastic

investigation of the PPET ionomers indicates that these new ionomers have very strong ionic associations with long association lifetimes at low ionic concentrations.<sup>27</sup> Consequently, fewer phosphonate ions may be available to interact with the polyamide at concentrations below 0.5 mol %, as compared to the more weakly interacting sulfonate ions. Future rheological comparisons between PPET and SPET, on an equal mol % ion basis, will be required to confirm this consideration.

At concentrations approaching 0.5 mol % of pendant ions, it becomes apparent that the phosphonate ions are interacting more effectively with the polyamide as compared to the sulfonate ions. The pendant ion concentration at the rapid decline in phase dimensions for  $\text{Na}^+$ -PPET/PETG/MXD6 blends is about 3 times smaller than that for  $\text{Na}^+$ -SPET ionomer-containing blends. This implies, at the same mol % of pendant ions, that the phosphonate ions are 3 times more effective at compatibilizing PETG/MXD6 blends compared to the sulfonate pendant ions. The specific interactions generated by phosphonate pendant ions are presumably much stronger than that for sulfonate pendant ions; thus, phosphonate pendant ions are more effective in compatibilizing polyester/polyamide blends.

## CONCLUSION

In this work, we have demonstrated the successful compatibilization of PETG/MXD6 blends using a new  $\text{Na}^+$ -PPET ionomer as a minor-component compatibilizer and confirmed that the divalent phosphonate pendant ion is more effective at compatibilizing polyester/polyamide blends in comparison to the monovalent sulfonate pendant ions. Melt-treated  $\text{Na}^+$ -PPET/PETG/MXD6 blend films show a phase-separated spinodal structure by PC-OM analysis and a distinct scattering halo by SALLS characterization. The interdomain spacing has been characterized by measurement from the PC-OM images and calculation by SALLS. With respect to the mol % of phosphonated monomer, the interdomain spacing decreases greatly with increasing mol % of ionic monomer at low functional monomer concentration (i.e., below 0.0133 mol %), then reaches a plateau in the range of 0.0133–0.233 mol %, and finally undergoes a rapid decline above 0.233 mol %, followed by the loss of a detectable phase morphology. The compatibilization effect of monovalent sulfonate and divalent phosphonate pendant ions has been compared with respect to mol % of ionic monomers and mol % of pendant ions, respectively. The comparison on a mol % of ionic monomers basis demonstrates the  $\text{Na}^+$ -PPET/PETG/MXD6 blends require 6 times fewer ionic monomers to achieve the same compatibility of polyester/polyamide blends relative to blends compatibilized with the conventional SPET ionomer. On a per mol pendant ion basis, the phosphonate ions have been found to be 3 times more effective at compatibilizing polyester/polyamide blends relative to sulfonate ions. Given the superior compatibilization effect for the divalent phosphonate pendant ions,  $\text{Na}^+$ -PPET ionomer is an attractive compatibilizer for various polyester/polyamide blend systems. Future systematic investigations will be focused on the compatibilization of polyester/polyamide melt blends using the  $\text{Na}^+$ -PPET ionomer for packaging applications.

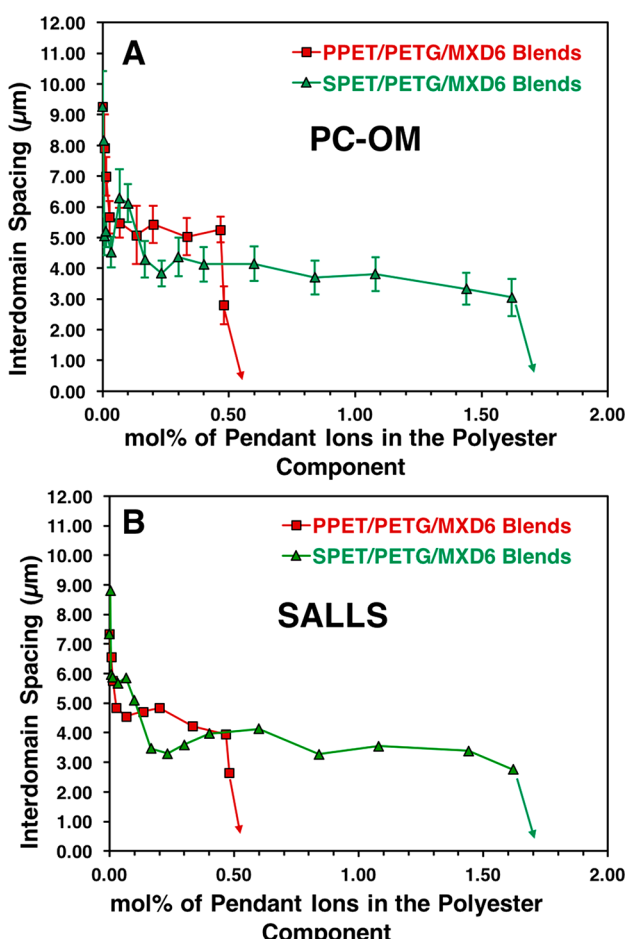


**Figure 9.** Interdomain spacing with respect to mol % of pendant ions in the polyester component for the  $\text{Na}^+$ -SPET/PETG/MXD6 and  $\text{Na}^+$ -PPET/PETG/MXD6 blends based on (A) measured values from the phase contrast optical microscopy (PC-OM) images and (B) calculated values from small-angle laser light scattering (SALLS).

## ASSOCIATED CONTENT

### Supporting Information

The Supporting Information is available free of charge on the [ACS Publications website](#) at DOI: [10.1021/acsapm.9b00097](https://doi.org/10.1021/acsapm.9b00097).

Thermal properties; interdomain spacing distribution (measured from PC-OM images) for  $\text{Na}^+$ -PPET/PETG/MXD6 blends; the plot of interdomain spacing (measured from PC-OM images) for  $\text{Na}^+$ -PPET/PETG/MXD6 blends; FTIR spectra; interdomain spacing versus time for blends of 75/25 (w/w %) PETG/MXD6, 50/50 (w/w %) PETG/MXD6, 75 (0.0667)/25, and 75 (0.233)25 at 240 °C; interdomain spacing of base blend at different anneal temperatures; PC-OM images, interdomain spacing distribution, and SALLS patterns of  $\text{Na}^+$ -SPET/PETG/MXD6 blends ([PDF](#))

## AUTHOR INFORMATION

### Corresponding Author

\*E-mail [rbmoore3@vt.edu](mailto:rbmoore3@vt.edu).

### ORCID

Lin Ju: [0000-0001-6393-4853](https://orcid.org/0000-0001-6393-4853)

Timothy E. Long: [0000-0001-9515-5491](https://orcid.org/0000-0001-9515-5491)

Robert B. Moore: [0000-0001-9057-7695](https://orcid.org/0000-0001-9057-7695)

### Notes

The authors declare no competing financial interest.

## ACKNOWLEDGMENTS

The authors gratefully acknowledge the Institute for Advanced Learning and Research (IALR) for providing funds to support the efforts of this project. This material is based, in part, upon work supported by the National Science Foundation under Grant DMR-1809291.

## REFERENCES

- (1) Iyer, S.; Schiraldi, D. A. Role of Ionic Interactions in the Compatibility of Polyester Ionomers with Poly (ethylene terephthalate) and Nylon 6. *J. Polym. Sci., Part B: Polym. Phys.* **2006**, *44*, 2091–2103.
- (2) Lee, R.; Hutchinson, G.; Farha, S.; Tharmapuram, S. Compatibilized Polyester/Polyamide Blends. U.S. Patent Application No. 10/395899.
- (3) Özén, İ.; Bozkulu, G.; Dalgıçdır, C.; Yücel, O.; Ünsal, E.; Çakmak, M.; Menceloglu, Y. Z. Improvement in Gas Permeability of Biaxially Stretched PET Films Blended with High Barrier Polymers: The Role of Chemistry and Processing Conditions. *Eur. Polym. J.* **2010**, *46*, 226–237.
- (4) Pratipati, V.; Hu, Y.; Bandi, S.; Schiraldi, D.; Hiltner, A.; Baer, E.; Mehta, S. Effect of Compatibilization on the Oxygen Barrier Properties of Poly (ethylene terephthalate)/Poly (*m* xylylene adipamide) Blends. *J. Appl. Polym. Sci.* **2005**, *97*, 1361–1370.
- (5) Turner, S. R.; Connell, G. W.; Stafford, S. L.; Hewa, J. D. Polyester-Polyamide Blends with Reduced Gas Permeability and Low Haze. U.S. Patent 6444283.
- (6) Hu, Y.; Pratipati, V.; Mehta, S.; Schiraldi, D.; Hiltner, A.; Baer, E. Improving Gas Barrier of PET by Blending with Aromatic Polyamides. *Polymer* **2005**, *46*, 2685–2698.
- (7) Bell, E. T.; Bradley, J. R.; Long, T. E.; Stafford, S. L. Polyester/Polyamide Blends with Improved Color. U.S. Patent 6239233.
- (8) Pratipati, V.; Hu, Y.; Bandi, S.; Mehta, S.; Schiraldi, D.; Hiltner, A.; Baer, E. Improving the Transparency of Stretched Poly (ethylene terephthalate)/Polyamide Blends. *J. Appl. Polym. Sci.* **2006**, *99*, 225–235.
- (9) Lundberg, R. D. 12 Elastomers and Fluid Applications. *Ionomers: Synthesis, Structure, Properties and Applications* **1997**, 477.
- (10) Tant, M. R.; Mauritz, K. A.; Wilkes, G. L. *Ionomers: Synthesis, Structure, Properties and Applications*; Springer Science & Business Media: 2012.
- (11) Zhang, L.; Brostowitz, N. R.; Cavicchi, K. A.; Weiss, R. Perspective: Ionomer Research and Applications. *Macromol. React. Eng.* **2014**, *8*, 81–99.
- (12) Boykin, T. L.; Moore, R. B. The Role of Specific Interactions and Transreactions on the Compatibility of Polyester Ionomers with Poly (ethylene terephthalate) and Nylon 6, 6. *Polym. Eng. Sci.* **1998**, *38*, 1658–1665.
- (13) Dutta, D.; Weiss, R.; He, J. Compatibilization of Blends Containing Thermotropic Liquid Crystalline Polymers with Sulfonate Ionomers. *Polymer* **1996**, *37*, 429–435.
- (14) Eisenberg, A.; Hara, M. A Review of Miscibility Enhancement via Ion Dipole Interactions. *Polym. Eng. Sci.* **1984**, *24*, 1306–1311.
- (15) Rajagopalan, P.; Kim, J. S.; Brack, H. P.; Lu, X.; Eisenberg, A.; Weiss, R.; Risen, W. M., Jr. Molecular Interpretation of Miscibility in Polyamide 6 Blends with Alkali Ionomers of Sulfonated Polystyrene. *J. Polym. Sci., Part B: Polym. Phys.* **1995**, *33*, 495–503.
- (16) Feng, Y.; Weiss, R.; Karim, A.; Han, C.; Ankner, J. F.; Kaiser, H.; Peiffer, D. G. Compatibilization of Polymer Blends by Complexation. 2. Kinetics of Interfacial Mixing. *Macromolecules* **1996**, *29*, 3918–3924.
- (17) Hara, M.; Eisenberg, A. Miscibility Enhancement via Ion-Dipole Interactions. 1. Polystyrene Ionomer/Poly (Alkylene Oxide) Systems. *Macromolecules* **1984**, *17*, 1335–1340.
- (18) Gemeinhardt, G. C.; Moore, A. A.; Moore, R. B. Influence of Ionomeric Compatibilizers on the Morphology and Properties of Amorphous Polyester/Polyamide Blends. *Polym. Eng. Sci.* **2004**, *44*, 1721–1731.
- (19) Sullivan, M.; Weiss, R. Characterization of Blends of An Amorphous Polyamide with Lightly Sulfonated Polystyrene Ionomers. *Polym. Eng. Sci.* **1992**, *32*, 517–523.
- (20) Samios, C. K.; Kalfoglou, N. K. Compatibilization of Poly (ethylene terephthalate)/Polyamide-6 Alloys: Mechanical, Thermal and Morphological Characterization. *Polymer* **1999**, *40*, 4811–4819.
- (21) Ng, C.-W. A.; MacKnight, W. J. Ionomeric Blends of Poly (ethyl acrylate-*co*-4-vinylpyridine) with Metal-Neutralized Sulfonated Poly (ethylene terephthalate). 4. Effects of Counterions. *Macromolecules* **1996**, *29*, 2421–2429.
- (22) Feng, Y.; Schmidt, A.; Weiss, R. Compatibilization of Polymer Blends by Complexation. 1. Spectroscopic Characterization of Ion-Amide Interactions in Ionomer/Polyamide Blends. *Macromolecules* **1996**, *29*, 3909–3917.
- (23) Goh, S.; Lee, S.; Zhou, X.; Tan, K. X-ray Photoelectron Spectroscopic Studies of Interactions between Poly (4-vinylpyridine) and Poly (styrenesulfonate) Salts. *Macromolecules* **1998**, *31*, 4260–4264.
- (24) Lu, X.; Weiss, R. Specific Interactions and Miscibility of Blends of Poly (*ε*-caprolactam) and Sulfonated PEEK Ionomer. *J. Polym. Sci., Part B: Polym. Phys.* **1996**, *34*, 1795–1807.
- (25) Wu, Q.; Weiss, R. Viscoelastic Properties of Poly (styrene-*co*-vinylphosphonate) Ionomers. *Polymer* **2007**, *48*, 7558–7566.
- (26) Zhuang, H.; Pearce, E. M.; Kwei, T. Self-association in Poly (styrene-*co*-4-vinylbenzenephosphonic acid) and Miscibility of its Blends. *Polymer* **1995**, *36*, 2237–2241.
- (27) Ju, L.; Pretelt, J.; Chen, T.; Dennis, J. M.; Heifferon, K. V.; Baird, D. G.; Long, T. E.; Moore, R. B. Synthesis and Characterization of Phosphonated Poly (ethylene terephthalate) Ionomers. *Polymer* **2018**, *151*, 154–163.
- (28) Orler, E. B.; Moore, R. B. Influence of Ionic Interactions on the Crystallization of Lightly Sulfonated Syndiotactic Polystyrene Ionomers. *Macromolecules* **1994**, *27*, 4774–4780.
- (29) Stein, R.; Misra, A. Morphological Studies on Polybutylene Terephthalate. *J. Polym. Sci., Polym. Phys. Ed.* **1980**, *18*, 327–342.

(30) Hanes, M. D. Blends of Poly(ethylene terephthalate) and Monovinylarene/Conjugated Diene Block Copolymers. U.S. Patent 5756578.

(31) Landis, F. A.; Moore, R. B. Blends of a Perfluorosulfonate Ionomer with Poly (vinylidene fluoride): Effect of Counterion Type on Phase Separation and Crystal Morphology. *Macromolecules* **2000**, *33*, 6031–6041.

(32) Nishimoto, M.; Keskkula, H.; Paul, D. Role of Slow Phase Separation in Assessing the Equilibrium Phase Behaviour of PC-PMMA Blends. *Polymer* **1991**, *32*, 272–278.

(33) Yang, J. C.; Kyu, T. Kinetics of Phase Separation of Nafion Perfluorinated Ionomer and Poly (vinylidene fluoride) Blends. *Macromolecules* **1990**, *23*, 182–186.

(34) Kyu, T.; Yang, J. C. Miscibility Studies of Perfluorinated Nafion Ionomer and Poly (vinylidene fluoride) Blends. *Macromolecules* **1990**, *23*, 176–182.

(35) Stein, R. S.; Rhodes, M. B. Photographic Light Scattering by Polyethylene Films. *J. Appl. Phys.* **1960**, *31*, 1873–1884.

(36) Hashimoto, T.; Izumitani, T. Effect of A Block Copolymer on the Kinetics of Spinodal Decomposition of Polymer Blends. 1. Nonuniversality in Scaled Characteristic Quantities versus Reduced Time. *Macromolecules* **1993**, *26*, 3631–3638.

(37) Lu, X.; Weiss, R. Development of Miscible Blends of Polyamide-6 and Manganese Sulfonated Polystyrene Using Specific Interactions. *Macromolecules* **1991**, *24*, 4381–4385.

(38) Pike, S. J.; Hutchinson, J. J.; Hunter, C. A. H-Bond Acceptor Parameters for Anions. *J. Am. Chem. Soc.* **2017**, *139*, 6700–6706.

(39) Feng, Y.; Weiss, R.; Han, C. Compatibilization of Polymer Blends by Complexation. 3. Structure Pinning during Phase Separation of Ionomer/Polyamide Blends. *Macromolecules* **1996**, *29*, 3925–3930.

(40) Tucker, R.; Han, C. C.; Dobrynin, A. V.; Weiss, R. A. Small-Angle Neutron Scattering Analysis of Blends with Very Strong Intermolecular Interactions: Polyamide/Ionomer Blends. *Macromolecules* **2003**, *36*, 4404–4410.

(41) Eisenberg, A.; Hird, B.; Moore, R. A New Multiplet-Cluster Model for the Morphology of Random Ionomers. *Macromolecules* **1990**, *23*, 4098–4107.